Arch Appl Mech (2007) 77: 689–696
DOI 10.1007/s00419-007-0126-0

ORIGINAL

J. S. Yang · Z. G. Chen · Y. T. Hu · S. N. Jiang · S. H. Guo

Propagation of thickness-twist waves in a multi-sectioned piezoelectric plate of 6 mm crystals

Received: 21 September 2006 / Accepted: 2 February 2007 / Published online: 6 March 2007

Abstract We study thickness-twist vibrations and waves in an unbounded, multi-sectioned piezoelectric plate of crystals with 6 mm symmetry or polarized ceramics. An exact solution from the three-dimensional equations of piezoelectricity is obtained. Basic vibration and wave propagation characteristics are calculated based on the solution. The results are useful in the understanding and design of plate resonators, filters and acoustic wave sensors of ZnO, AlN and polarized ceramics.

Keywords Piezoelectricity · Plate · Wave · Vibration

1 Introduction

Thickness-twist vibration modes are anti-plane or shear horizontal (SH) modes in plates. Thickness-twist modes of crystal plates are often used as the operating modes for resonators, filters and acoustic wave sensors [1–5] made from quartz [1–4] and polarized ceramics [5]. Recently, thin AlN and ZnO films are of growing interest because of the development of thin-film resonators [6,7]. They are crystals of 6 mm symmetry. Plates with normal, in-plane or tilted sixfold axes are all being developed [8]. When the sixfold axis of a 6 mm crystal is parallel to the major surfaces of a plate, thickness-twist waves can propagate in an unbounded plate [5]. For a finite rectangular plate of 6 mm crystals with in-plane poling, thickness-twist modes have also been shown to exist [9]. The results of [9] allow us to analyze thickness-twist modes in an unbounded, multi-sectioned piezoelectric plate of 6 mm crystals (see Fig. 1). The sixfold axis is along the x_3 axis. The material of each portion is different from those of the neighboring portions. The structure may be considered as an example of the so-called functionally graded (FGM) materials which may exhibit interesting and useful phenomena and are of growing interest.

It is has been known for a long time that the motion of a mobile charge in a crystal is governed by Schroedinger's equation with a periodic potential, and the resulting eigenvalue spectrum has band structures that can describe conduction and semiconduction. Mathematically this is a consequence of the variable coefficients in the differential equation and therefore it allows other physical interpretations, e.g., the propagation of acoustic waves in periodically structured phononic crystals approximately governed by differential equations with

J. S. Yang · Z. G. Chen · Y. T. Hu (✉) · S. N. Jiang · S. H. Guo
Institute of Mechanics and Sensing Technology,
School of Civil Engineering and Architecture, Central South University, Changsha, Hunan 410083, China
E-mail: hudeng@263.net

J. S. Yang
Department of Engineering Mechanics, University of Nebraska, Lincoln, NE 68588-0526, USA

Y. T. Hu
Department of Mechanics, School of Civil Engineering and Mechanics,
Huazhong University of Science and Technology, Wuhan, Hubei 430074, China

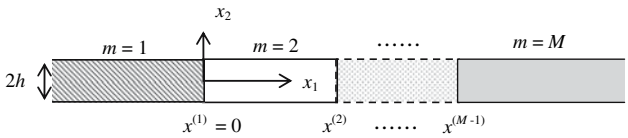

Fig. 1 An inhomogeneous piezoelectric plate of 6 mm crystals or polarized ceramics

variable coefficients or by equations with piecewise constant, alternating coefficients [10–13]. The study of phononic crystals has led to results with potentials for new and useful acoustic wave devices. In the analysis of phononic crystals, usually an elastic analysis is performed without piezoelectric coupling. The periodic structures of the composite, two- or multi-phase phononic crystals are represented by differential equations with smooth and periodic coefficients, which is of an approximate or averaged nature [15].

In this paper we present a piezoelectric analysis of thickness-twist vibrations and propagating waves in the structure in Fig. 1. An exact solution satisfying the three-dimensional equations of linear piezoelectricity is obtained in spite of the complexity of the coupled electromechanical fields. Since the material tensors of polarized ceramics which are transversely isotropic have the same structures as those of crystals of 6 mm symmetry [14], our analysis is also valid for polarized ceramics. Our work is different from [13] which studies extensional waves in a multi-sectioned rod. Our analysis is two dimensional and is exact while [13] uses the approximate one-dimensional equation for extension. The solution obtained allows us to calculate the basic vibration characteristics of the structure in Fig. 1 and exhibit a few interesting and useful behaviors.

2 Governing equations

Consider the plate in Fig. 1. The plate is unelectroded. The major surfaces are traction-free. Thickness-twist modes are governed by

$$\begin{aligned} &u_1 = u_2 = 0, \\ &u_3 = u(x_1, x_2, t), \quad \phi = \phi(x_1, x_2, t), \end{aligned} \tag{1}$$

where $\mathbf{u}$ is the displacement vector and ϕ is the electric potential. In a typical section of the plate, the m-th, a function ψ can be introduced through $\phi = \psi + e^{(m)}u/\varepsilon^{(m)}$ [5,9] where $e^{(m)} = e_{15}^{(m)}$ and $\varepsilon^{(m)} = \varepsilon_{11}^{(m)}$ are the relevant piezoelectric and dielectric constants of the section. The governing equations for u and ψ are [5,9]:

$$\bar{c}^{(m)}\nabla^2 u = \rho^{(m)}\ddot{u}, \quad \nabla^2\psi = 0, \tag{2}$$

where ∇^2 is the two-dimensional Laplacian, $\bar{c}^{(m)} = c^{(m)} + (e^{(m)})^2/\varepsilon^{(m)}$, and $c^{(m)} = c_{44}^{(m)}$ is the relevant elastic constant. The first of Eq. (2) is Newton's law of motion. The second of Eq. (2) is the charge equation (Gauss's law of electrostatics). The nonzero stress components are the shear stress components T_{31} and T_{32}, and the nonzero electric displacement components are the in-plane components D_1 and D_2 [5,9]. They are given by

$$\begin{aligned} &T_{23} = \bar{c}^{(m)}u_{,2} + e^{(m)}\psi_{,2}, \quad T_{31} = \bar{c}^{(m)}u_{,1} + e^{(m)}\psi_{,1}, \\ &D_1 = -\varepsilon^{(m)}\psi_{,1}, \quad D_2 = -\varepsilon^{(m)}\psi_{,2}, \end{aligned} \tag{3}$$

where an index after a comma denotes partial differentiation with respect to the coordinate associated with the index. For unelectroded and traction-free surfaces, $T_{23} = 0$ and $D_2 = 0$ at $x_2 = \pm h$, which describes that the traction and free charge vanish at $x_2 = \pm h$. Or, equivalently, in terms of u and ψ,

$$u_{,2} = 0, \quad \psi_{,2} = 0, \quad x_2 = \pm h. \tag{4}$$

3 An exact solution

It can be verified by separation of variables [9] or direct substitution that the solutions to Eqs. (2) and (4) can be classified into waves anti-symmetric or symmetric in x_2. They are given by

$$\begin{aligned} u^{(m,n)} &= [A^{(m,n)} \exp(i\xi_1^{(m,n)} x_1) + B^{(m,n)} \exp(-i\xi_1^{(m,n)} x_1)] \sin \xi_2^{(n)} x_2 \exp(i\omega t), \\ \psi^{(m,n)} &= [C^{(m,n)} \exp(\xi_2^{(n)} x_1) + D^{(m,n)} \exp(-\xi_2^{(n)} x_1)] \sin \xi_2^{(n)} x_2 \exp(i\omega t), \\ \xi_2^{(n)} &= \frac{n\pi}{2h}, \quad n = 1, 3, 5, \ldots, \end{aligned} \tag{5}$$

and

$$\begin{aligned} u^{(m,n)} &= [A^{(m,n)} \exp(i\xi_1^{(m,n)} x_1) + B^{(m,n)} \exp(-i\xi_1^{(m,n)} x_1)] \cos \xi_2^{(n)} x_2 \exp(i\omega t), \\ \psi^{(m,n)} &= [C^{(m,n)} \exp(\xi_2^{(n)} x_1) + D^{(m,n)} \exp(-\xi_2^{(n)} x_1)] \cos \xi_2^{(n)} x_2 \exp(i\omega t), \\ \xi_2^{(n)} &= \frac{n\pi}{2h}, \quad n = 0, 2, 4, \ldots, \end{aligned} \tag{6}$$

where

$$\begin{aligned} \xi_1^{(m,n)} &= \sqrt{\frac{\rho^{(m)}\omega^2}{\bar{c}^{(m)}} - (\xi_2^{(n)})^2} \\ &= \sqrt{\frac{\rho^{(m)}}{\bar{c}^{(m)}}} \sqrt{\omega^2 - \left(\frac{n\pi}{2h}\right)^2 \frac{\bar{c}^{(m)}}{\rho^{(m)}}} = \frac{1}{v_T^{(m)}} \sqrt{\omega^2 - (\omega^{(m,n)})^2}, \\ v_T^{(m)} &= \sqrt{\frac{\bar{c}^{(m)}}{\rho^{(m)}}}, \quad (\omega^{(m,n)})^2 = \left(\frac{n\pi}{2h}\right)^2 \frac{\bar{c}^{(m)}}{\rho^{(m)}}. \end{aligned} \tag{7}$$

In Eqs. (5) and (6), $A^{(m,n)}$, $B^{(m,n)}$, $C^{(m,n)}$ and $D^{(m,n)}$ are undetermined constants. Equation (5) has a sine dependence on x_2 and Eq. (6) has a cosine dependence. In particular, the mode with $n = 0$ in Eq. (6) is independent of x_2 and is called a face-shear mode. Face-shear is the simplest mode and its behavior is similar to the extensional waves studied in [13], and therefore will be excluded in the analysis below.

Consider the anti-symmetric modes in Eq. (5) first. To apply the interface continuity conditions at the junctions between two neighboring sections, we calculate

$$\begin{aligned} \phi^{(m,n)} &= \left[\frac{e^{(m)}}{\varepsilon^{(m)}} A^{(m,n)} \exp(i\xi_1^{(m,n)} x_1) + \frac{e^{(m)}}{\varepsilon^{(m)}} B^{(m,n)} \exp(-i\xi_1^{(m,n)} x_1)\right. \\ &\qquad \left. + C^{(m,n)} \exp(\xi_2^{(n)} x_1) + D^{(m,n)} \exp(-\xi_2^{(n)} x_1)\right] \sin \xi_2^{(n)} x_2 \exp(i\omega t), \\ D_1^{(m,n)} &= \left[-\varepsilon^{(m)} C^{(m,n)} \xi_2^{(n)} \exp(\xi_2^{(n)} x_1) + \varepsilon^{(m)} D^{(m,n)} \xi_2^{(n)} \exp(-\xi_2^{(n)} x_1)\right] \sin \xi_2^{(n)} x_2 \exp(i\omega t), \\ T_{13}^{(mn)} &= \left[\bar{c}^{(m)} A^{(m,n)} i\xi_1^{(m,n)} \exp(i\xi_1^{(m,n)} x_1) - \bar{c}^{(m)} B^{(m,n)} i\xi_1^{(m,n)} \exp(-i\xi_1^{(m,n)} x_1)\right. \\ &\qquad \left. + e^{(m)} C^{(m,n)} \xi_2^{(n)} \exp(\xi_2^{(n)} x_1) - e^{(m)} D^{(m,n)} \xi_2^{(n)} \exp(-\xi_2^{(n)} x_1)\right] \sin \xi_2^{(n)} x_2 \exp(i\omega t). \end{aligned} \tag{8}$$

At the m-th interface with $x_1 = x^{(m)}$ between the m-th portion and the $(m+1)$-th portion, we have the continuity of the displacement, potential and traction, and there is no free charge at the interface:

$$\begin{aligned} u^{(m,n)}(x_1 = x^{(m)-}) &= A^{(m,n)} \exp(i\xi_1^{(m,n)} x^{(m)}) + B^{(m,n)} \exp(-i\xi_1^{(m,n)} x^{(m)}) \\ &= A^{(m+1,n)} \exp(i\xi_1^{(m+1,n)} x^{(m)}) + B^{(m+1,n)} \exp(-i\xi_1^{(m+1,n)} x^{(m)}) \\ &= u^{(m+1,n)}(x_1 = x^{(m)+}), \end{aligned} \tag{9}$$

$$\begin{aligned}
\phi^{(m,n)}(x_1 = x^{(m)-}) &= \frac{e^{(m)}}{\varepsilon^{(m)}} A^{(m,n)} \exp(i\xi_1^{(m,n)} x^{(m)}) + \frac{e^{(m)}}{\varepsilon^{(m)}} B^{(m,n)} \exp(-i\xi_1^{(m,n)} x^{(m)}) \\
&\quad + C^{(m,n)} \exp(\xi_2^{(n)} x^{(m)}) + D^{(m,n)} \exp(-\xi_2^{(n)} x^{(m)}) \\
&= \frac{e^{(m+1)}}{\varepsilon^{(m+1)}} A^{(m+1,n)} \exp(i\xi_1^{(m+1,n)} x^{(m)}) + \frac{e^{(m+1)}}{\varepsilon^{(m+1)}} B^{(m+1,n)} \exp(-i\xi_1^{(m+1,n)} x^{(m)}) \\
&\quad + C^{(m+1,n)} \exp(\xi_2^{(n)} x^{(m)}) + D^{(m+1,n)} \exp(-\xi_2^{(n)} x^{(m)}) = \phi^{(m+1,n)}(x_1 = x^{(m)+}), \qquad (10) \\
T_{13}^{(m,n)}(x_1 = x^{(m)-}) &= \bar{c}^{(m)} A^{(m,n)} i\xi_1^{(m,n)} \exp(i\xi_1^{(m,n)} x^{(m)}) - \bar{c}^{(m)} B^{(m,n)} i\xi_1^{(m,n)} \exp(-i\xi_1^{(m,n)} x^{(m)}) \\
&\quad + e^{(m)} C^{(m,n)} \xi_2^{(n)} \exp(\xi_2^{(n)} x^{(m)}) - e^{(m)} D^{(m,n)} \xi_2^{(n)} \exp(-\xi_2^{(n)} x^{(m)}) \\
&= \bar{c}^{(m+1)} A^{(m+1,n)} i\xi_1^{(m+1,n)} \exp(i\xi_1^{(m+1,n)} x^{(m)}) \\
&\quad - \bar{c}^{(m+1)} B^{(m+1,n)} i\xi_1^{(m+1,n)} \exp(-i\xi_1^{(m+1,n)} x^{(m)}) \\
&\quad + e^{(m+1)} C^{(m+1,n)} \xi_2^{(n)} \exp(\xi_2^{(n)} x^{(m)}) - e^{(m+1)} D^{(m+1,n)} \xi_2^{(n)} \\
&\quad \times \exp(-\xi_2^{(n)} x^{(m)}) \\
&= T_{13}^{(m+1,n)}(x_1 = x^{(m)+}), \qquad (11) \\
D_1^{(m,n)}(x_1 = x^{(m)-}) &= -\varepsilon^{(m)} C^{(m,n)} \xi_2^{(n)} \exp(\xi_2^{(n)} x^{(m)}) + \varepsilon^{(m)} D^{(m,n)} \xi_2^{(n)} \exp(-\xi_2^{(n)} x^{(m)}) \\
&= -\varepsilon^{(m+1)} C^{(m+1,n)} \xi_2^{(n)} \exp(\xi_2^{(n)} x^{(m)}) + \varepsilon^{(m+1)} D^{(m+1,n)} \xi_2^{(n)} \\
&\quad \times \exp(-\xi_2^{(n)} x^{(m)}) = D_1^{(m+1,n)}(x_1 = x^{(m)+}), \qquad (12)
\end{aligned}$$

where a factor of $\sin \xi_2^{(n)} x_2 \exp(i\omega t)$ has been dropped. Equations (9–12) can be written in the following matrix form:

$$\begin{aligned}
&\begin{bmatrix}
\exp(i\xi_1^{(m,n)} x^{(m)}) & \exp(-i\xi_1^{(m,n)} x^{(m)}) & 0 & 0 \\
\frac{e^{(m)}}{\varepsilon^{(m)}} \exp(i\xi_1^{(m,n)} x^{(m)}) & \frac{e^{(m)}}{\varepsilon^{(m)}} \exp(-i\xi_1^{(m,n)} x^{(m)}) & \exp(\xi_2^{(n)} x^{(m)}) & \exp(-\xi_2^{(n)} x^{(m)}) \\
\bar{c}^{(m)} i\xi_1^{(m,n)} \exp(i\xi_1^{(m,n)} x^{(m)}) & -\bar{c}^{(m)} i\xi_1^{(m,n)} \exp(-i\xi_1^{(m,n)} x^{(m)}) & e^{(m)} \xi_2^{(n)} \exp(\xi_2^{(n)} x^{(m)}) & -e^{(m)} \xi_2^{(n)} \exp(-\xi_2^{(n)} x^{(m)}) \\
0 & 0 & -\varepsilon^{(m)} \xi_2^{(n)} \exp(\xi_2^{(n)} x^{(m)}) & \varepsilon^{(m)} \xi_2^{(n)} \exp(-\xi_2^{(n)} x^{(m)})
\end{bmatrix} \\
&\quad \times \begin{Bmatrix} A^{(m,n)} \\ B^{(m,n)} \\ C^{(m,n)} \\ D^{(m,n)} \end{Bmatrix} \\
&= \begin{bmatrix}
\exp(i\xi_1^{(m+1,n)} x^{(m)}) & \exp(-i\xi_1^{(m+1,n)} x^{(m)}) & 0 & 0 \\
\frac{e^{(m+1)}}{\varepsilon^{(m+1)}} \exp(i\xi_1^{(m+1,n)} x^{(m)}) & \frac{e^{(m+1)}}{\varepsilon^{(m+1)}} \exp(-i\xi_1^{(m+1,n)} x^{(m)}) & \exp(\xi_2^{(n)} x^{(m)}) & \exp(-\xi_2^{(n)} x^{(m)}) \\
\bar{c}^{(m+1)} i\xi_1^{(m+1,n)} \exp(i\xi_1^{(m+1,n)} x^{(m)}) & -\bar{c}^{(m+1)} i\xi_1^{(m+1,n)} \exp(-i\xi_1^{(m+1,n)} x^{(m)}) & e^{(m+1)} \xi_2^{(n)} \exp(\xi_2^{(n)} x^{(m)}) & -e^{(m+1)} \xi_2^{(n)} \exp(-\xi_2^{(n)} x^{(m)}) \\
0 & 0 & -\varepsilon^{(m+1)} \xi_2^{(n)} \exp(\xi_2^{(n)} x^{(m)}) & \varepsilon^{(m+1)} \xi_2^{(n)} \exp(-\xi_2^{(n)} x^{(m)})
\end{bmatrix} \\
&\quad \times \begin{Bmatrix} A^{(m+1,n)} \\ B^{(m+1,n)} \\ C^{(m+1,n)} \\ D^{(m+1,n)} \end{Bmatrix}. \qquad (13)
\end{aligned}$$

In matrix and vector notation, Eq. (13) can be written as

$$[\mathbf{T}]_{x^{(m)}}^{(m,n)} \{\mathbf{F}\}^{\{m,n\}} = [\mathbf{T}]_{x^{(m)}}^{(m+1,n)} \{\mathbf{F}\}^{\{m+1,n\}}, \qquad (14)$$

where

$$[\mathbf{T}]_x^{(m,n)} = \begin{bmatrix}
\exp(i\xi_1^{(m,n)} x) & \exp(-i\xi_1^{(m,n)} x) & 0 & 0 \\
\frac{e^{(m)}}{\varepsilon^{(m)}} \exp(i\xi_1^{(m,n)} x) & \frac{e^{(m)}}{\varepsilon^{(m)}} \exp(-i\xi_1^{(m,n)} x) & \exp(\xi_2^{(n)} x) & \exp(-\xi_2^{(n)} x) \\
\bar{c}^{(m)} i\xi_1^{(m,n)} \exp(i\xi_1^{(m,n)} x) & -\bar{c}^{(m)} i\xi_1^{(m,n)} \exp(-i\xi_1^{(m,n)} x) & e^{(m)} \xi_2^{(n)} \exp(\xi_2^{(n)} x) & -e^{(m)} \xi_2^{(n)} \exp(-\xi_2^{(n)} x) \\
0 & 0 & -\varepsilon^{(m)} \xi_2^{(n)} \exp(\xi_2^{(n)} x) & \varepsilon^{(m)} \xi_2^{(n)} \exp(-\xi_2^{(n)} x)
\end{bmatrix}, \qquad (15)$$

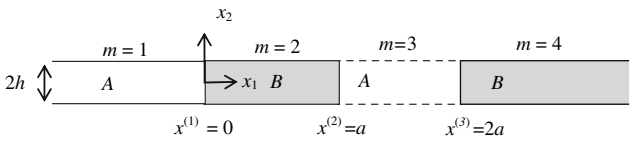

Fig. 2 A four-sectioned plate

$$\{\mathbf{F}\}^{(m,n)} = \begin{Bmatrix} A^{(m,n)} \\ B^{(m,n)} \\ C^{(m,n)} \\ D^{(m,n)} \end{Bmatrix}. \tag{16}$$

Equation (14) can be further written as

$$\begin{aligned} \{\mathbf{F}\}^{(m+1,n\}} &= [\mathbf{K}]^{(m,n)}\{\mathbf{F}\}^{(m,n\}}, \\ [\mathbf{K}]^{(m,n)} &= \left([\mathbf{T}]^{(m+1,n)}_{x^{(m)}}\right)^{-1}[\mathbf{T}]^{(m,n)}_{x^{(m)}}. \end{aligned} \tag{17}$$

Suppose that the structure has M sections. With Eq. (17) we can write

$$\{\mathbf{F}\}^{(M,n\}} = [\mathbf{K}]^{(M-1,n)}[\mathbf{K}]^{(M-2,n)}\cdots[\mathbf{K}]^{(2,n)}[\mathbf{K}]^{(1,n)}\{\mathbf{F}\}^{(1,n\}}. \tag{18}$$

Equation (18) is a relation between the fields in the first and the last sections. It has four component equations for $A^{(1,n)}$, $B^{(1,n)}$, $C^{(1,n)}$, $D^{(1,n)}$, $A^{(M,n)}$, $B^{(M,n)}$, $C^{(M,n)}$ and $D^{(M,n)}$.

For the symmetric modes in Eq. (6), the result is the same except that n assumes even numbers.

4 Numerical results

The above formulation is rather general and allows us to analyze various problems of practical importance. We analyze two below.

4.1 Incident wave in a plate with four sections

First consider a plate of four sections as shown in Fig. 2. Two materials denoted by A and B are used alternatively. To be specific, we choose A and B to be PZT-7 and PZT-4, respectively. In this case

$$\omega_0^A = \frac{\pi}{2h}\sqrt{\frac{\bar{c}_A}{\rho_A}} < \frac{\pi}{2h}\sqrt{\frac{\bar{c}_B}{\rho_B}} = \omega_0^B, \tag{19}$$

which is the fundamental thickness-twist frequency ($n = 1$) of an unbounded plate. $h = 1$ mm. $a = b = 5$ mm. Thickness-twist waves have a fundamental difference from the extensional waves analyzed in [13] in that thickness-twist waves have cutoff frequencies but extensional waves do not. Below a certain frequency called the cutoff frequency, thickness-twist waves cannot propagate and decay exponentially. Equation (19) in fact gives the cutoff frequencies of the fundamental ($n = 1$) thickness-twist waves in the corresponding plates. The behavior of an incident thickness-twist wave in the four-sectioned plate in Fig. 2 depends strongly on its frequency as compared to ω_0^A and ω_0^B. We discuss the three possibilities separately. When an incident wave is coming from $x_1 = -\infty$ in the first portion, $B^{(1,n)}$ is known and $D^{(1,n)}$ can be chosen as zero for simplicity. The fields in the other sections may vary according to ω, ω_0^A and ω_0^B.

4.1.1 $\omega > \omega_0^B > \omega_0^A$

In this case, the wave can also propagate in material B. In the last section, there is a right-traveling wave only, with $A^{(M,n)} = 0$ and $C^{(M,n)} = 0$. Equation (18) can be used to solve for the reflected wave $A^{(1,n)}$ and $C^{(1,n)}$ in the first section, the transmitted wave $B^{(M,n)}$ and $D^{(M,n)}$ in the last section, and fields in every section of the

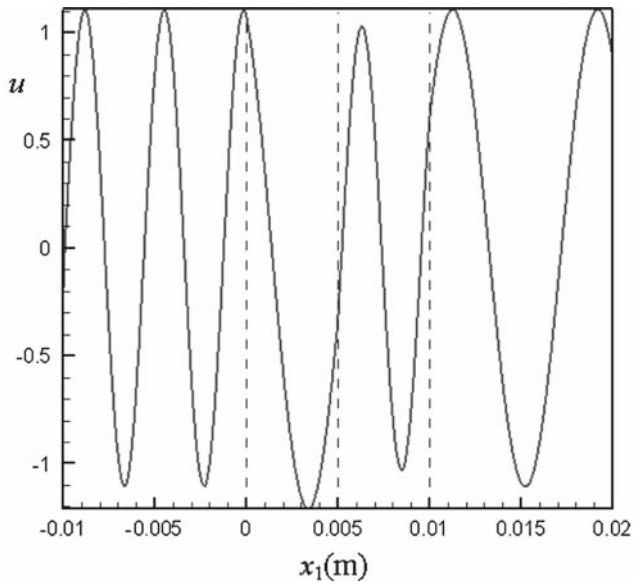

Fig. 3 Displacement distribution when $\omega = 1.12\omega_0^B$

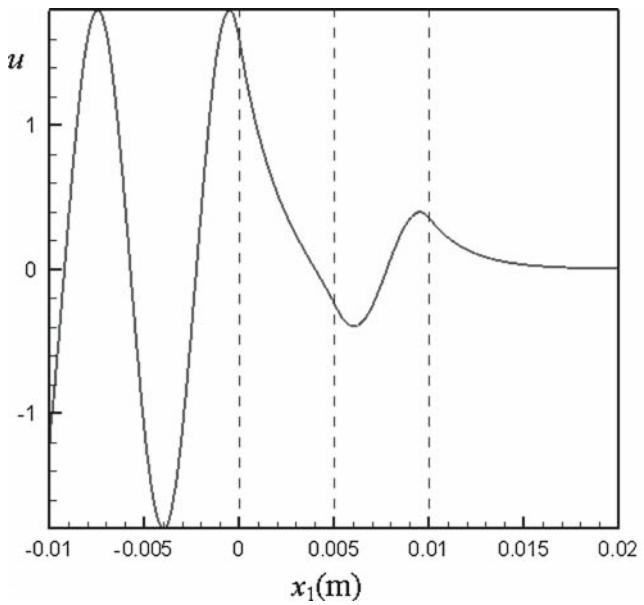

Fig. 4 Displacement distribution when $\omega = 0.95\omega_0^B$

structure. The displacement distribution along the plate is shown in Fig. 3. The four sections are separated by dotted lines. We have sinusoidal variations in all four sections, with different wavelengths in the two materials.

4.1.2 $\omega_0^B > \omega > \omega_0^A$

In this case, the wave can propagate in material A but not in material B. In the last section a decaying field when $x_1 \to \infty$ is allowed but the growing field should be discarded. Therefore we require that $B^{(M,n)} = 0$ and $C^{(M,n)} = 0$. Equation (18) can be used to solve for the reflected wave $A^{(1,n)}$ and $C^{(1,n)}$ in the first section, the decaying fields $A^{(M,n)}$ and $D^{(M,n)}$ in the last section, and fields in every section of the structure. The displacement distribution along the plate is shown in Fig. 4. The four sections are separated by dotted lines. We have sinusoidal variations in material A and exponential fields in material B.

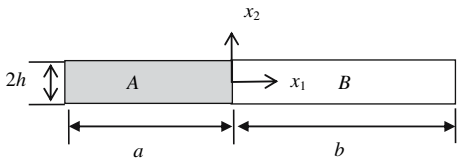

Fig. 5 Unit cell of a periodic plate

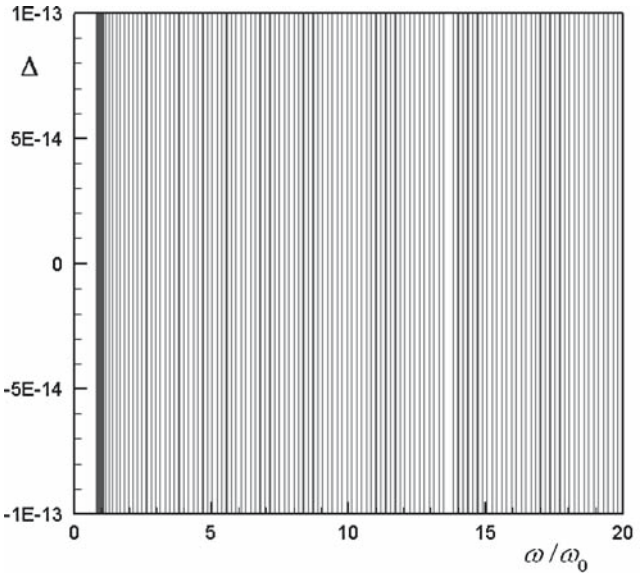

Fig. 6 Frequency spectrum of the periodic plate

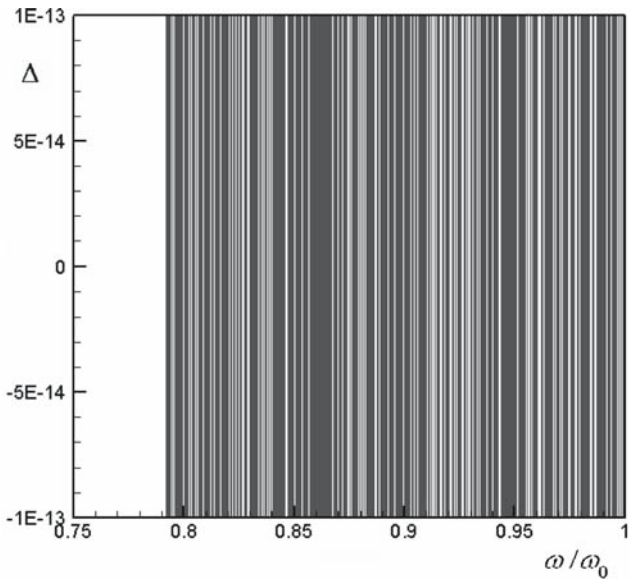

Fig. 7 Fine structure of the frequency spectrum of the periodic plate

4.1.3 $\omega_0^B > \omega_0^A > \omega$

In this case, the wave cannot propagate in both materials. We cannot specify an incident wave. Instead, we require the fields to be decaying when $x_1 \to \pm\infty$. We have an eigenvalue problem. These modes are not of much practical interest because the fields decay rapidly and there is not much vibration throughout the plate.

4.2 Modes in a periodic plate

Next we examine the frequency spectrum of modes in a period plate. In this case, it is sufficient to consider a two-portion unit cell (see Fig. 5). The periodic plate is obtained by repeating the unit sell in the x_1 direction and in unbounded. Material A is PZT-5H and B is PZ-34. $h = 1\,\text{mm}$, $a = b = 10\,\text{mm}$. The continuity conditions at the junction and periodic conditions at both ends lead to eight homogeneous equations representing an eigenvalue problem. For nontrivial solutions, the determinant of the coefficient matrix, denoted by Δ, has to vanish, which yields the frequency equation whose roots are the eigenvalues. We plot in Fig. 6 the curve of Δ versus frequency. The intersections of the curve with the horizontal axis are the eigenvalues. To see the intersections better, only the range of small Δ is shown. The intersections with the horizontal axes are discrete. They are dense at certain places and sparse at other places, showing band structures. Each thick line represents an eigenvalue band which in fact consists of many discrete roots. In particular, if we magnify the first wide band to the left of $\omega/\omega_0 = 1$, we see further detailed structures of the band as shown in Fig. 7. In both Figs. 6 and 7, the horizontal axis is normalized by $\omega_0 = \omega_0^B$ from PZ-34.

5 Conclusion

An exact theoretical analysis is performed for thickness-twist vibrations and waves in a multi-sectioned piezoelectric plate of polarized ceramics or 6 mm crystals, which is one of a few rare cases in which an exact solution can be obtained. Numerical results show that the behavior of thickness-twist waves in a multi-sectioned plate varies greatly according to the wave frequency and the cutoff frequencies of each section. A wave may propagate with a sinusoidal variation or decay exponentially. The eigenvalue spectrum of thickness-twist modes in a periodic plate of two or more materials have banded structures.

References

1. Mindlin, R.D.: Thickness-twist vibrations of an infinite, monoclinic, crystal plate. Int. J. Solids Struct. **1**(2), 141–145 (1965)
2. Mindlin, R.D.: Bechmann's number for harmonic overtones of thickness/twist vibrations of rotated Y-cut quartz plates. J. Acoust. Soc. Am. **41**(4), 969–973 (1967)
3. Pearman, G.T.: Thickness-twist vibrations in beveled AT-cut quartz plates. J. Acoust. Soc. Am. **45**(4), 928–934 (1968)
4. Bleustein, J.: Thickness-twist and face-shear vibrations of a contoured crystal plate. Int. J. Solids Struct. **2**(3), 351–360 (1966)
5. Bleustein, J.L.: Some simple modes of wave propagation in an infinite piezoelectric plate. J. Acoust. Soc. Am. **45**(3), 614–620 (1969)
6. Pang, W., Zhang, H., Kim, E.S.: Micromachined acoustic wave resonator isolated from substrate. IEEE Trans. Ultrason. Ferroelectr. Freq. Control **52**(8), 1239–1246 (2005)
7. Link, M., Schreiter, M., Weber, J., Primig, R., Pitzer, D., Cabl, R.: Solidly mounted ZnO shear mode film bulk acoustic wave resonators for sensing applications in liquids. IEEE Trans. Ultrason. Ferroelectr. Freq. Control **53**(2), 492–496 (2006)
8. Martin, F., Jan, M.-E., Rey-Mermet, S., Belgacem, B., Su, D., Cantoni, M., Muralt, P.: Shear Mode Coupling and Tilted Grain Growth of AlN Thin Films in BAW Resonators. IEEE Trans. Ultras. Ferroelectr. Freq. Control **53**(7), 1339–1343 (2006)
9. Yang, J.S., Guo, S.H.: Thickness-twist modes in a rectangular piezoelectric resonator of hexagonal crystals. Appl. Phys. Lett. **88**, 153506 (2006)
10. Laude, V., Wilm, M., Benchabane, S., Khelif, A.: Full band gaps for surface acoustic waves in piezoelectric phononic crystals. Ultrason. Symp. IEEE **2**, 1046–1049 (2004)
11. Huang, Z.-G., Wu, T.-T.: Temperature effect on the bandgaps of surface and bulk acoustic waves in two-dimensional phononic crystals. IEEE Trans. Ultrason. Ferroelectr. Freq. Control **52**(3), 365–370 (2005)
12. Hsieh, P.-F., Wu, T.-T., Sun, J.-H.: Three-dimensional phononic band gap calculations using FDTD method and a PC cluster system. IEEE Trans. Ultrason. Ferroelectr. Freq. Control **53**(1), 148–158 (2006)
13. Li, F.M., Wang, Y.S., Chen, A.L.: Wave localization in randomly disordered periodic rods. Acta Mechanica Solida Sinica **19**(1), 50–57 (2006)
14. Tiersten, H.F.: Linear Piezoelectric Plate Vibrations. Plenum, New York (1969)
15. Yang, J.S., Chen, Z.G., Hu, Y.T.: Trapped thickness-twist modes in an inhomogeneous piezoelectric plate of 6 mm crystals. Philos. Mag. Lett. **86**(11), 699–705 (2006)